Supporting Information for

Splitting of multiple hydrogen molecules by bioinspired diniobium metal complexes: a DFT study

Felipe Fantuzzi,[abc] Marco Antonio Chaer Nascimento[a]*, Bojana Ginovska,[b] R. Morris Bullock[b] and Simone Raugei[b]*

[a] Instituto de Química, Universidade Federal do Rio de Janeiro, Av. Athos da Silveira Ramos 149, 21941.909, Rio de Janeiro, Brazil.

[b] Center for Molecular Electrocatalysis, Pacific Northwest National Laboratory, Richland, WA 99352, USA.

[c] Institute for Inorganic Chemistry, Julius-Maximilians-Universität Würzburg, Am Hubland, 97074, Würzburg, Germany.

Table of Contents

S1. $[Nb_2(CH_3CN)_m]^{4+}$ Species in Neat Acetonitrile Solution

In this section, we discuss the most abundant $[Nb_2(CH_3CN)_m]^{4+}$ species present in acetonitrile solution. This was obtained by performing several geometry optimizations and hessian calculations on distinct $[Nb_2(CH_3CN)_m]^{4+}$ species, with *m* varying from 3 to 10. The calculations were performed using the NWChem 6.8 software[S1] at the density functional level of theory (DFT) adopting the B3LYP[S2] exchange and correlation hybrid functional, with the 6-31G* basis set[S3] for main group atoms combined with the Stuttgart RSC 1997 basis set and ECP for Nb.[S4] This combination of basis sets and ECP is, from now on, called as BS2. The solvation energies were obtained by applying the Solvation Model Based on Density (SMD)[S5] method. Images of 3D structures and plots of frontier Kohn-Sham molecular orbitals (MOs) were obtained using IQmol.[S6]

Figure S1 shows the free energy of complex formation (ΔG_b, 298 K) of $[Nb_2(CH_3CN)_m]^{4+}$ species in acetonitrile solution, following the reaction depicted in eq. s1 (concentration corrections are taken into account). From the results, we could identify that $[Nb_2(CH_3CN)_8]^{4+}$ is the most stable $[Nb_2(CH_3CN)_m]^{4+}$ species in neat acetonitrile solution.

$$\left[Nb_2(CH_3CN)_{10}\right]^{4+} \rightarrow \left[Nb_2(CH_3CN)_m\right]^{4+} + (10-m)CH_3CN \qquad (s1)$$

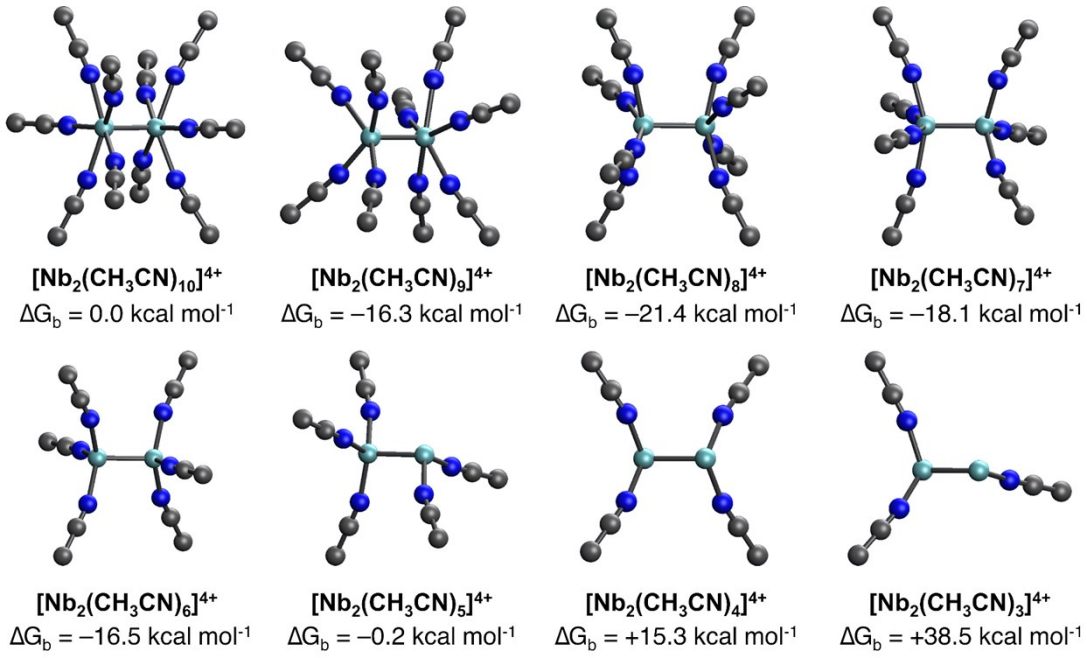

Figure S1. Optimized structures and free energy of complex formation (ΔG_b, 298.15 K) of $[Nb2(CH3CN)_m]^{4+}$ species in acetonitrile solution at the B3LYP/6-31G* level of theory. Spectator hydrogen atoms are omitted for clarity. The Nb–Nb bond distances are in the range of 2.38-2.41 Å.

Table S1. Thermochemistry of distinct $[Nb_2(CH_3CN)_m]^{4+}$ (m = 3-10) structures at the B3LYP/BS2+SMD(CH3CN)// B3LYP/BS2 level of theory. Concentration corrections for G were included.

Species	E (E_h)	G_{corr} (E_h)	G (E_h)	ΔG_b (kcal mol^{-1})
m = 10	-1441.257185	0.684554	-1440.572631	0.0
m = 9	-1308.473476	0.612258	-1307.861218	-16.3
m = 8	-1175.689512	0.557468	-1175.132044	-21.4
m = 7	-1042.880156	0.490631	-1042.389525	-18.1
m = 6	-910.073628	0.423897	-909.649731	-16.5
m = 5	-777.245740	0.359383	-776.886358	-0.2
m = 4	-644.418742	0.294397	-644.124345	+15.3
m = 3	-511.580179	0.230123	-511.350056	+38.5
MeCN	-132.7647261	0.027411071	-132.737315	-

S2. Thermochemistry and Charge Analysis of Selected Nb_2^{4+} Species

Table S2. Vertical electronic energies and vertical singlet-triplet (S-T) and singlet-quintet (S-Q) gaps of selected Nb_2^{4+} species at the B3LYP-D3(BJ)/def2-SVP level of theory.

Species	E-singlet (E_h)	E-triplet (E_h)	E-quintet (E_h)	S-T gap (kcal mol^{-1})	S-Q gap (kcal mol^{-1})
1a	-2017.625985	-2017.590631	-2017.516610	22.2	68.6
1b	-2017.612018	-2017.581657	-2017.533994	19.1	49.0
1c	-2017.606038	-2017.597937	-2017.561447	5.1	28.0
1d	-2017.598970	-2017.579093	-2017.528340	12.5	44.3
2	-2861.011766	-2860.950205	-2860.883544	38.6	80.5
2.H$_2$	-2862.250927	-2862.215532	-2862.166612	22.2	52.9
2.H$_4$	-2863.394987	-2863.364541	-2863.292865	19.1	64.1
2.H$_6$	-2864.603279	-2864.585388	-2864.494884	11.2	68.0
2.H$_8$	-2865.766532	-2865.725284	-2865.659862	25.9	66.9
3	-3704.311463	-3704.293139	-3704.220076	11.5	57.3
3.H$_2$	-3705.554866	-3705.534240	-3705.472079	12.9	51.9
3.H$_4$	-3706.727961	-3706.716886	-3706.640101	6.9	55.1
3.H$_6$	-3707.943308	-3707.902096	-3707.792529	25.9	94.6
3.H$_8$	-3709.120626	-3709.076133	-3708.962356	27.9	99.3
4	-4547.631519	-4547.613119	-4547.586678	11.5	28.1
4.H$_2$	-4548.876750	-4548.863536	-4548.827445	8.3	30.9
4.H$_4$	-4550.090771	-4550.056869	-4549.983197	21.3	67.5
4.H$_6$	-4551.294609	-4551.264625	-4551.176826	18.8	73.9
4.H$_8$	-4552.454819	-4552.410482	-4552.344372	27.8	69.3

Table S3. Thermochemistry (298.15 K) of selected Nb_2^{4+} species at the B3LYP-D3(BJ)/def2-TZVPP+PCM(MeCN)//B3LYP-D3(BJ)/def2-SVP and M06-D3/def2-TZVPP//B3LYP-D3(BJ)/def2-SVP levels of theory. Concentration corrections for G were included.

Species	E-B3LYP-D3(BJ) (E_h)	E-M06-D3 (E_h)	H_{corr} (E_h)	G_{corr} (E_h)
$P^{Me}{}_2N^{Me}{}_2$	-1109.359272	-1108.900011	0.293924	0.238466
MeCN	-132.824161	-132.718657	0.049627	0.026833
$[Nb_2(MeCN)_8]^{4+}$	-1176.220970	-1175.258148	0.411340	0.289817
H_2	-1.180145	-1.171061	0.013363	0.001582
1a	-2019.993569	-2018.763206	0.612357	0.479164
1b	-2019.969667	-2018.742312	0.609999	0.474021
1c	-2019.971508	-2018.744845	0.607406	0.477835
1d	-2019.958660	-2018.731369	0.611096	0.472622
2	-2863.775332	-2862.282304	0.809006	0.669251
2.1	-2730.916783	-2729.526217	0.756300	0.633353
2.2	-2732.095597	-2730.698772	0.772777	0.651709
2.3	-2732.139791	-2730.741748	0.773353	0.650914
2.H_2	-2864.998952	-2863.498989	0.825690	0.686542
2.H_4	-2866.135776	-2864.633158	0.837419	0.687491
2.H_6	-2867.339862	-2865.822393	0.864337	0.717231
2.H_8	-2868.501252	-2866.978763	0.880427	0.733633
3	-3707.471167	-3705.727136	1.003413	0.854024
3.H_2	-3708.706041	-3706.951388	1.020012	0.866927
3.H_4	-3709.873979	-3708.111991	1.034690	0.881406
3.H_6	-3711.084567	-3709.314230	1.058087	0.906331
3.H_8	-3712.259276	-3710.480066	1.078330	0.922772
4	-4551.190020	-4549.191065	1.201400	1.042896
4.H_2	-4552.427923	-4550.418699	1.216884	1.058227
4.H_4	-4553.636331	-4551.621666	1.230341	1.069116
4.H_6	-4554.841703	-4552.817881	1.256078	1.094901
4.H_8	-4556.010300	-4553.976984	1.280242	1.121159

Table S4. Free energy of complex formation, ΔG_b (kcal mol^{-1}), following eq. 1 at the B3LYP-D3(BJ)/def2-TZVPP+PCM(MeCN)//B3LYP-D3(BJ)/def2-SVP and M06-D3/def2-TZVPP//B3LYP-D3(BJ)/def2-SVP levels of theory. Concentration corrections for G were included. Values relative to **2**, herein referred as $\Delta(\Delta G_b)$, are also shown. Values for structures of the **3b** family, with $[Nb_2(P^{Me}{}_2N^{Me}{}_2)_3(H_2)_k]^{4+}$ stoichiometries, are also reported.

Species	ΔG_b, B3LYP-D3(BJ) (kcal mol^{-1})	$\Delta(\Delta G_b)$, B3LYP-D3(BJ) (kcal mol^{-1})	ΔG_b, M06-D3 (kcal mol^{-1})	$\Delta(\Delta G_b)$, M06-D3 (kcal mol^{-1})
2	-77.0	0.0	-55.8	0.0
2.1	-61.1	+15.9	-38.0	+17.8
2.2	-49.7	+27.3	-28.4	+27.4
2.3	-77.9	-1.0	-55.9	-0.1
2.H$_2$	-94.4	-17.4	-74.6	-18.8
2.H$_4$	-67.6	+9.4	-51.8	+4.0
2.H$_6$	-64.9	+12.0	-45.6	+10.2
2.H$_8$	-43.9	+33.1	-27.0	+28.8
3	-67.5	+9.5	-44.6	+11.2
3.H$_2$	-94.7	-17.8	-70.9	-15.1
3.H$_4$	-79.0	-2.0	-56.2	-0.4
3.H$_6$	-83.4	-6.5	-61.1	-5.3
3.H$_8$	-70.7	6.3	-48.5	+7.3
3b	-45.3	+31.6	-15.0	+40.9
3b.H$_2$	-67.3	+9.7	-38.7	+17.1
3b.H$_4$	-65.7	+11.2	-36.7	+19.1
3b.H$_6$	-66.5	+10.5	-39.7	+16.1
3b.H$_8$	-64.6	+12.3	-38.0	+17.8
4	-69.9	+7.1	-42.8	+13.0
4.H$_2$	-97.5	-20.6	-69.7	-13.9
4.H$_4$	-109.4	-32.4	-83.9	-28.1
4.H$_6$	-110.0	-33.1	-84.5	-28.7
4.H$_8$	-87.3	-10.4	-61.5	-5.7

Table S5. Hirshfeld atomic charges[S7] at the B3LYP-D3(BJ)/def2-TZVPP level of theory, obtained using the Multiwfn 3.7 software.[S8] The Nb labels indicate their order of appearance in the cartesian coordinates list (see section S13). The remaining values are the average Hirshfeld atomic charges of hydridic (H (Nb–H)) and protic (H (N–H)) hydrogen atoms in each structure.

Species	Nb1	Nb2	H (Nb–H)	H (N–H)
2	+0.30	+0.30	-	-
2.H$_2$	+0.41	+0.41	–0.15	-
2.H$_4$	+0.48	+0.48	–0.13	-
2.H$_6$	+0.34	+0.34	–0.15	+0.11
2.H$_8$	+0.35	+0.36	–0.14	+0.11
3	+0.29	+0.39	-	-
3.H$_2$	+0.37	+0.43	–0.14	-
3.H$_4$	+0.38	+0.50	–0.13	-
3.H$_6$	+0.32	+0.46	–0.14	+0.11
3.H$_8$	+0.31	+0.43	–0.15	+0.10
4	+0.24	+0.21	-	-
4.H$_2$	+0.38	+0.43	–0.14	-
4.H$_4$	+0.38	+0.38	–0.11	-
4.H$_6$	+0.24	+0.26	–0.13	+0.11
4.H$_8$	+0.13	+0.21	–0.15	+0.10

S3. Screening of Molecular Structures

Around 200 structures containing the Nb_2^{4+} core and distinct numbers of acetonitrile (CH_3CN) solvent molecules (from 0 to 4), diphosphine ($P^{Me}{}_2N^{Me}{}_2$) ligands (from 1 to 4) and H atoms (from 0 to 8) were pre-optimized at the B3LYP/BS2 level of theory following the procedure described in section S1. Hessian calculations were performed for all stationary states in the range of 0-50 kcal mol^{-1} from the least energetic structure of each chemical formula. This molecular screening allowed us to identify all potential candidates for the main discussion of this work. Selected low-lying structures are presented in the next sections.

S4. $[Nb_2(CH_3CN)_4(P^{Me}{}_2N^{Me}{}_2)_2]^{4+}$ Isomers

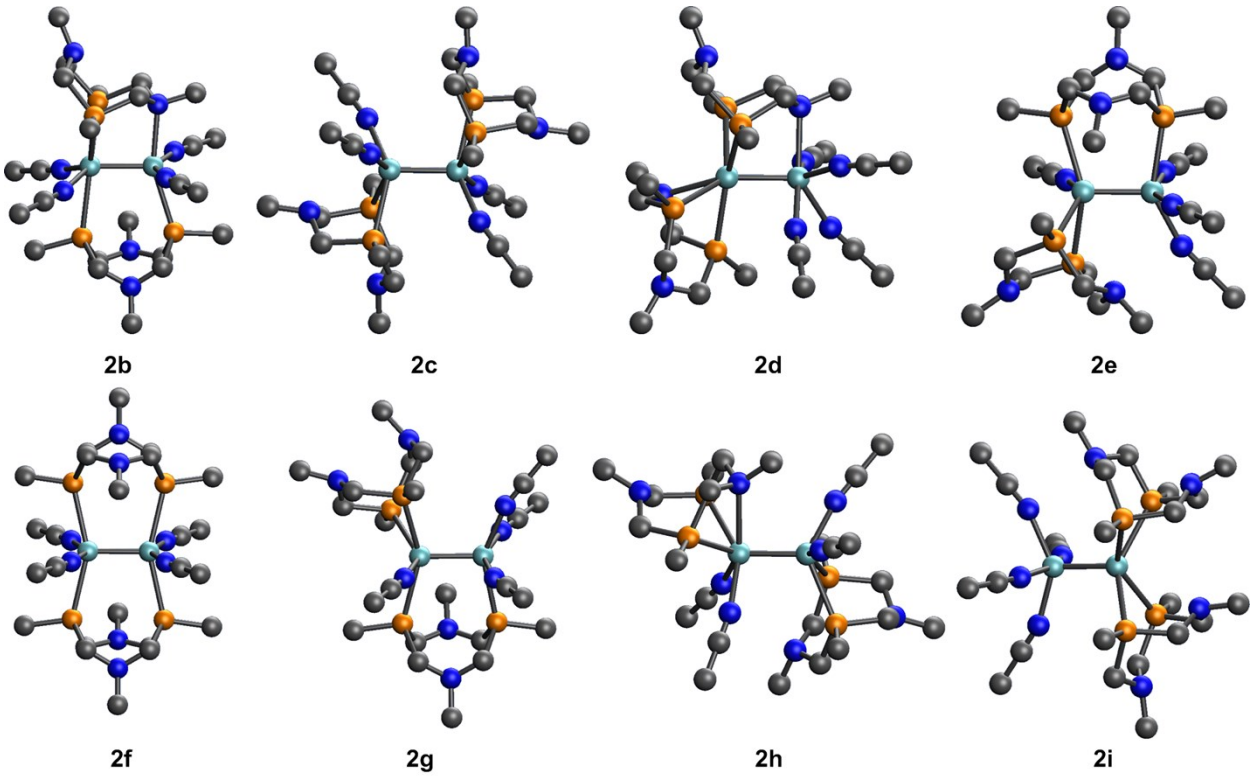

Figure S2. Ranking of low-lying free energy isomers (**2b**-**2i**) of $[Nb_2(CH_3CN)_4(P^{Me}{}_2N^{Me}{}_2)_2]^{4+}$ calculated in acetonitrile at the B3LYP/BS2+SMD(CH3CN)//B3LYP/BS2 level of theory. Spectator hydrogen atoms are omitted for clarity.

Table S6. Thermochemistry of distinct $[Nb_2(CH_3CN)_4(P^{Me}{}_2N^{Me}{}_2)_2]^{4+}$ isomers at the B3LYP/BS2+SMD(CH3CN)// B3LYP/BS2 level of theory. Concentration corrections were taken into account.

Species	E (E_h)	G_{corr} (E_h)	G (E_h)	ΔG (kcal mol^{-1})
2	–2862.828275	0.673314	-2862.154961	0.0
2b	–2862.803500	0.671368	-2862.132132	+14.3
2c	–2862.790622	0.661423	-2862.129199	+16.2
2d	–2862.792008	0.669120	-2862.122888	+20.1
2e	–2862.785638	0.665785	-2862.119853	+22.0
2f	–2862.775046	0.660143	-2862.114903	+25.1
2g	–2862.774543	0.661046	-2862.113498	+26.0
2h	–2862.773802	0.663431	-2862.110371	+28.0
2i	–2862.773656	0.666923	-2862.106733	+30.3

S5. $[Nb_2(CH_3CN)_4(P^{Me}{}_2N^{Me}{}_2)_2(H_2)]^{4+}$ Isomers

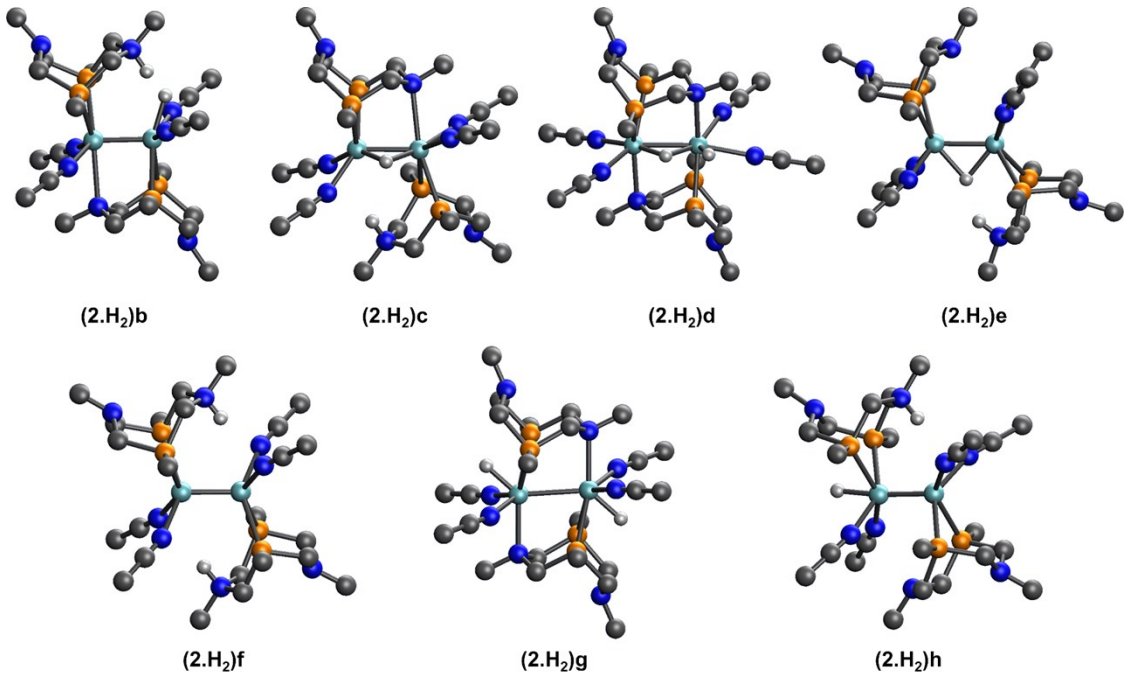

Figure S3. (2.H_2)b: optimized structure at the B3LYP(D3BJ)/def2-SVP level of theory. **(2.H_2)c** to **(2.H_2)h** : ranking of low-lying free energy isomers of $[Nb_2(CH_3CN)_4(P^{Me}{}_2N^{Me}{}_2)_2H_2]^{4+}$ calculated in acetonitrile at the B3LYP/BS2+SMD(CH3CN)// B3LYP/BS2 level of theory. Spectator hydrogen atoms are omitted for clarity.

Table S7. Thermochemistry of distinct $[Nb_2(CH_3CN)_4(P^{Me}{}_2N^{Me}{}_2)_2H_2]^{4+}$ isomers. Concentration corrections for G were included.

B3LYP-D3(BJ)/def2-TZVPP+PCM(MeCN)//B3LYP-D3(BJ)/def2-SVP				
Species	**E (E_h)**	**G_{corr} (E_h)**	**G (E_h)**	**ΔG (kcal mol^{-1})**
2.H_2	-2864.998952	0.686542	-2864.312410	0.0
(2.H_2)b	-2864.929024	0.692265	-2864.236759	+47.5
B3LYP/BS2+SMD(MeCN)// B3LYP/BS2				
Species	**E (E_h)**	**G_{corr} (E_h)**	**G (E_h)**	**ΔG (kcal mol^{-1})**
2.H_2	–2864.050678	0.689510	-2863.361168	0.0
(2.H_2)c	–2864.011135	0.689680	-2863.321456	+24.9
(2.H_2)d	–2864.004388	0.687305	-2863.317083	+27.7
(2.H_2)e	–2863.990805	0.679778	-2863.311027	+31.5
(2.H_2)f	–2863.992374	0.686276	-2863.306098	+34.6
(2.H_2)g	–2863.965091	0.691708	-2863.273383	+55.1
(2.H_2)h	–2863.943633	0.683003	-2863.260630	+63.1

S6. $[Nb_2(CH_3CN)_4(P^{Me}{}_2N^{Me}{}_2)_2(H_2)_2]^{4+}$ Isomers

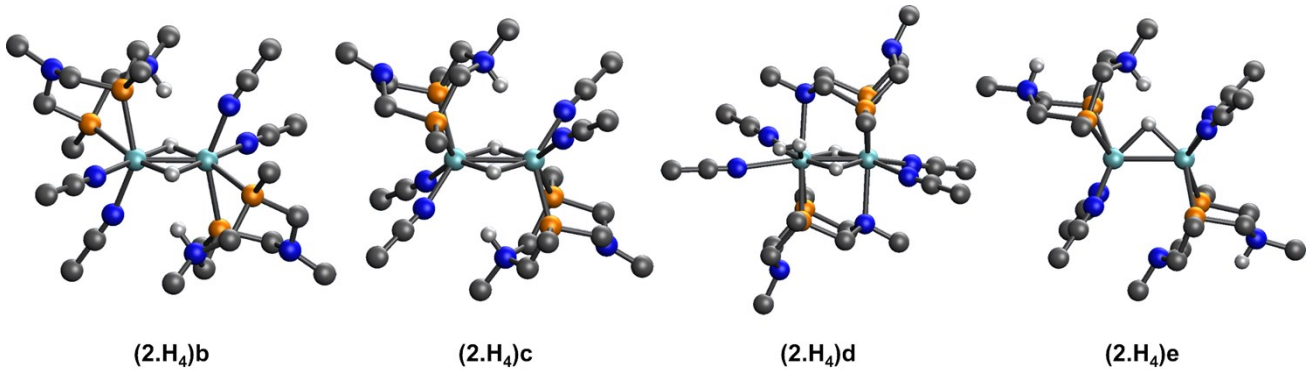

Figure S4. Ranking of low-lying free energy isomers of $[Nb_2(CH_3CN)_4(P^{Me}{}_2N^{Me}{}_2)_2H_4]^{4+}$ calculated in acetonitrile at the B3LYP/BS2+SMD(CH3CN)// B3LYP/BS2 level of theory. Spectator hydrogen atoms are omitted for clarity.

Table S8. Thermochemistry of distinct $[Nb_2(CH_3CN)_4(P^{Me}{}_2N^{Me}{}_2)_2(H_2)_2]^{4+}$ isomers at the B3LYP/BS2+SMD(CH3CN)// B3LYP/BS2 level of theory. Concentration corrections for G were included.

Species	E (E_h)	G_{corr} (E_h)	G (E_h)	ΔG (kcal mol^{-1})
2.H_4	–2865.199827	0.694280	-2864.505547	0.0
(2.H_4)b	–2865.206132	0.705111	-2864.501021	+2.8
(2.H_4)c	–2865.192313	0.702146	-2864.490167	+9.7
(2.H_4)d	–2865.189778	0.705551	-2864.484227	+13.4
(2.H_4)e	–2865.138840	0.710168	-2864.428672	+48.2

S7. $[Nb_2(CH_3CN)_4(P^{Me}{}_2N^{Me}{}_2)_2(H_2)_3]^{4+}$ Isomers

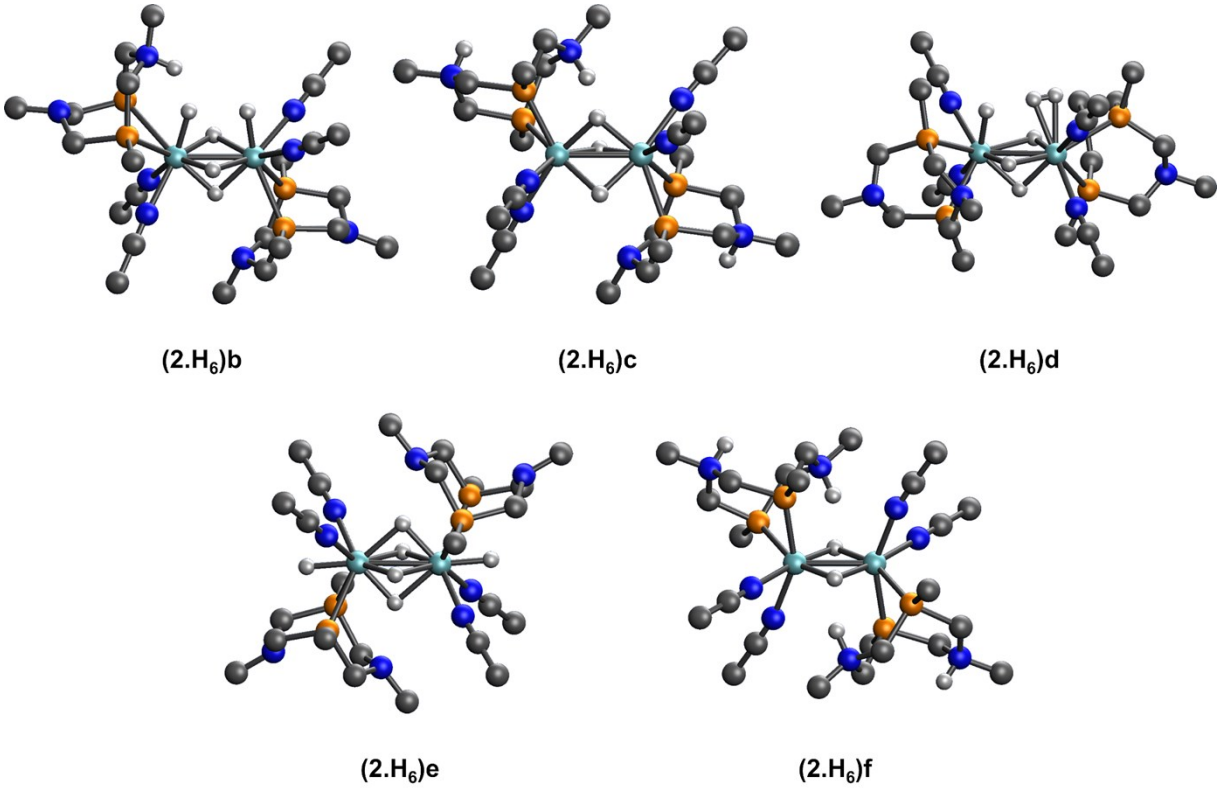

Figure S5. Ranking of low-lying free energy isomers of $[Nb_2(CH_3CN)_4(P^{Me}{}_2N^{Me}{}_2)_2(H_2)_3]^{4+}$ calculated in acetonitrile at the B3LYP/BS2+SMD(CH3CN)// B3LYP/BS2 level of theory. Spectator hydrogen atoms are omitted for clarity.

Table S9. Thermochemistry of distinct $[Nb_2(CH_3CN)_4(P^{Me}{}_2N^{Me}{}_2)_2H_6]^{4+}$ isomers at the B3LYP/BS2+SMD(CH3CN)// B3LYP/BS2 level of theory. Concentration corrections for G were included.

Species	E (E_h)	G_{corr} (E_h)	G (E_h)	ΔG (kcal mol^{-1})
2.H6	–2866.408349	0.722839	-2865.685510	0.0
(2.H6)b	–2866.371671	0.716593	-2865.655077	+19.1
(2.H6)c	–2866.371420	0.726231	-2865.645188	+25.3
(2.H6)d	–2866.346292	0.710543	-2865.635749	+31.2
(2.H6)e	–2866.327103	0.712482	-2865.614621	+44.5
(2.H6)f	–2866.338579	0.731700	-2865.606879	+49.3

S8. [$Nb_2(CH_3CN)_4(P^{Me}{}_2N^{Me}{}_2)_2(H_2)_4]^{4+}$ Isomers

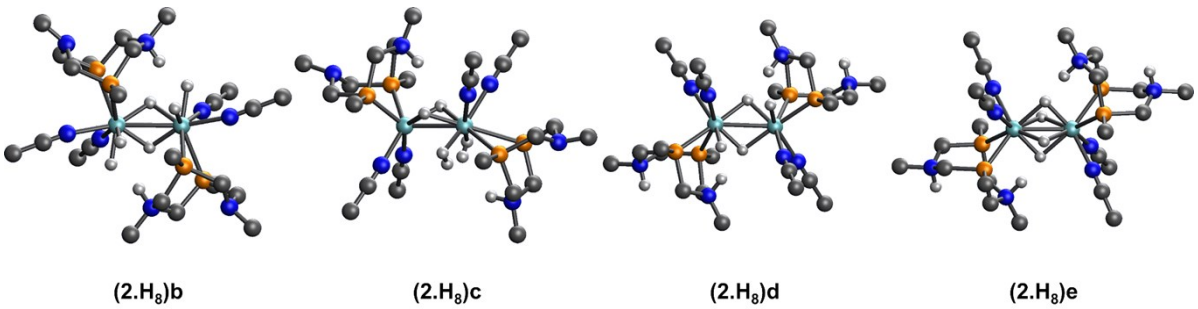

Figure S6. Ranking of low-lying free energy isomers of $[Nb_2(CH_3CN)_4(P^{Me}{}_2N^{Me}{}_2)_2H_8]^{4+}$ calculated in acetonitrile at the B3LYP/BS2+SMD(CH3CN)// B3LYP/BS2 level of theory. Spectator hydrogen atoms are omitted for clarity.

Table S10. Thermochemistry of distinct $[Nb_2(CH_3CN)_4(P^{Me}{}_2N^{Me}{}_2)_2(H_2)_4]^{4+}$ isomers at the B3LYP/BS2+SMD(CH3CN)// B3LYP/BS2 level of theory. Concentration corrections for G were included.

Species	E (E_h)	G_{corr} (E_h)	G (E_h)	ΔG (kcal mol^{-1})
2.H_8	–2867.554984	0.736036	-2866.818948	0.0
(2.H_8)b	–2867.561958	0.744554	-2866.817404	+1.0
(2.H_8)c	–2867.513745	0.736855	-2866.776890	+26.4
(2.H_8)d	–2867.521527	0.745230	-2866.776297	+26.8
(2.H_8)e	–2867.514067	0.744337	-2866.769730	+30.9

S9. $[Nb_2(P^{Me}{}_2N^{Me}{}_2)_3(H_2)_k]^{4+}$ (k = 1,2) Isomers

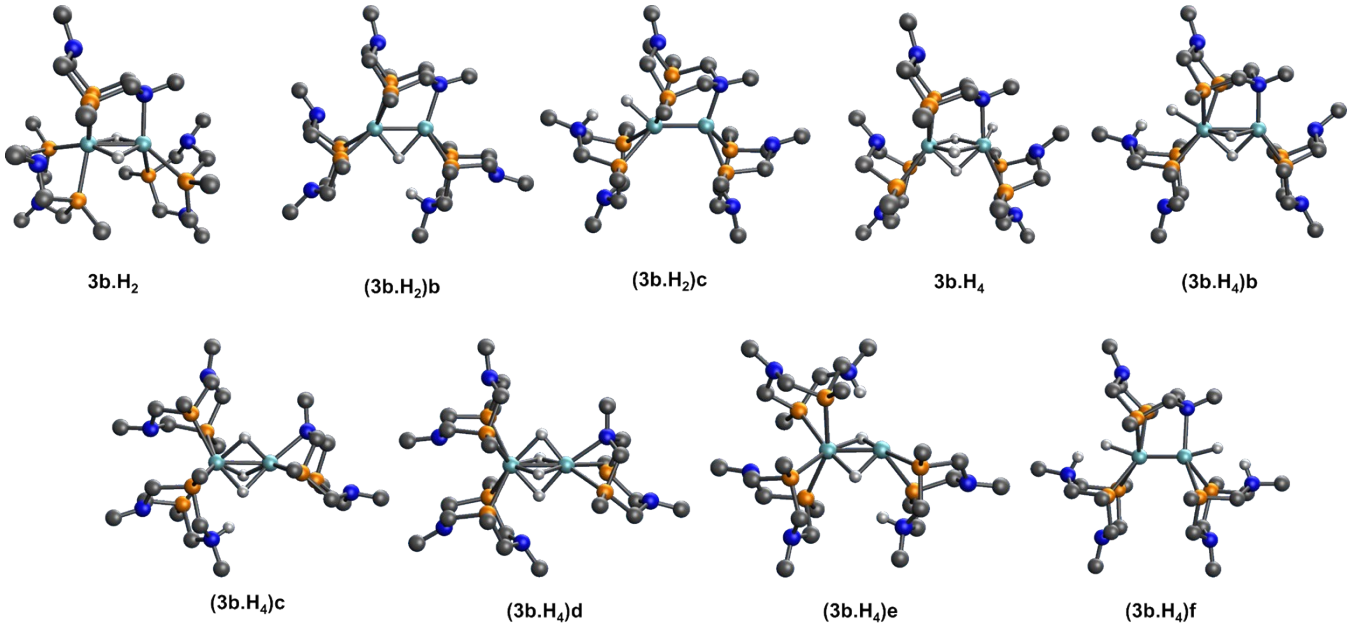

Figure S7. Ranking of low-lying free energy isomers of $[Nb_2(P^{Me}{}_2N^{Me}{}_2)_3(H_2)_k]^{4+}$ (k = 1,2) calculated in acetonitrile at the B3LYP/BS2+SMD(CH3CN)//B3LYP/BS2 level of theory. Spectator hydrogen atoms are omitted for clarity.

Table S11. Thermochemistry of distinct $[Nb_2(P^{Me}{}_2N^{Me}{}_2)_3H_k]^{4+}$ (k = 2,4) isomers at the B3LYP/BS2+SMD(CH3CN)// B3LYP/BS2 level of theory. Concentration corrections for G were included.

Species	E (E_h)	G_{corr} (E_h)	G (E_h)	ΔG (kcal mol^{-1})
3b.H_2	–3441.978737	0.784173	-3441.194564	0.0
(3b.H_2)b	–3441.978837	0.793896	-3441.184941	+6.0
(3b.H_2)c	–3441.941737	0.791960	-3441.149777	+28.1
3b.H_4	–3443.167906	0.806658	-3442.361248	0.0
(3b.H_4)b	–3443.167352	0.809295	-3442.358057	+2.0
(3b.H_4)c	–3443.157797	0.805789	-3442.352009	+5.8
(3b.H_4)d	–3443.140976	0.799896	-3442.341080	+12.7
(3b.H_4)e	–3443.144919	0.810737	-3442.334183	+17.0
(3b.H_4)f	–3443.121987	0.818781	-3442.303206	+36.4

S10. $[Nb_2(P^{Me}{}_2N^{Me}{}_2)_3(H_2)_k]^{4+}$ (k = 3,4) Isomers

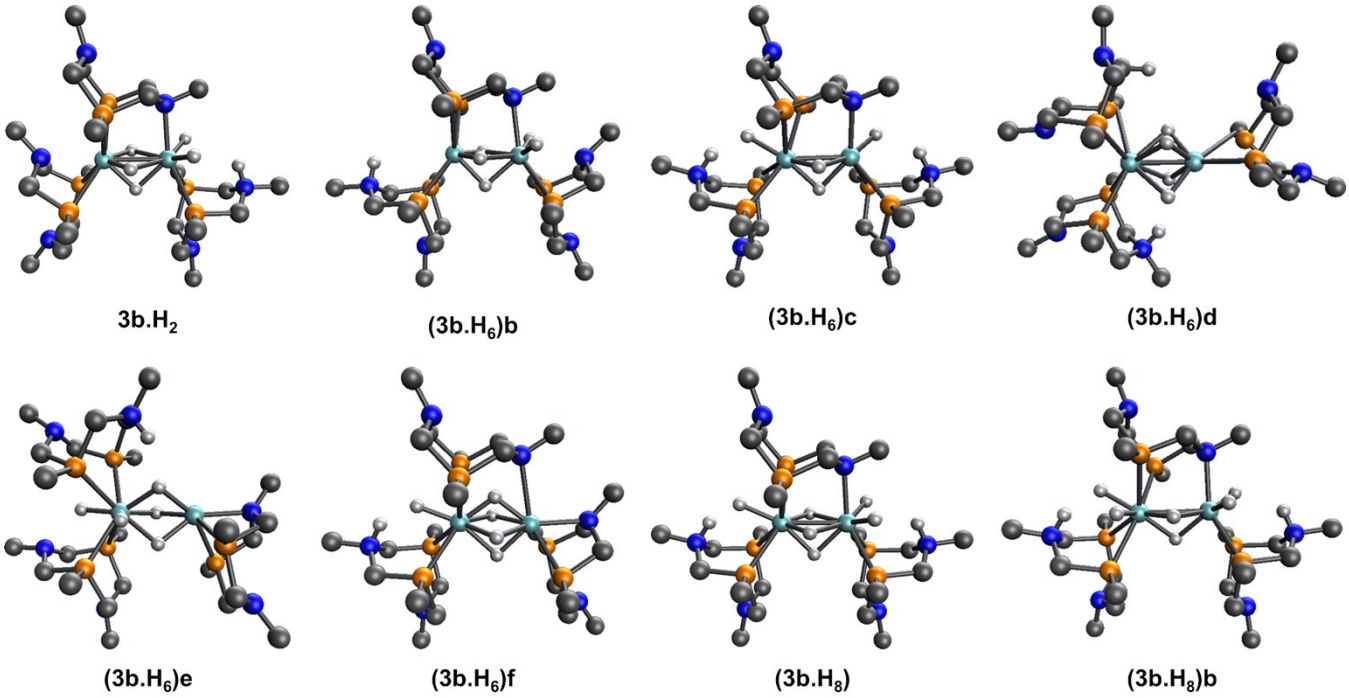

Figure S8. Ranking of low-lying free energy isomers of $[Nb_2(P^{Me}{}_2N^{Me}{}_2)_3(H_2)_k]^{4+}$ (k = 3,4) calculated in acetonitrile at the B3LYP/BS2+SMD(CH3CN)//B3LYP/BS2 level of theory. Spectator hydrogen atoms are omitted for clarity.

Table S12. Thermochemistry of distinct $[Nb_2(P^{Me}{}_2N^{Me}{}_2)_3(H_2)_k]^{4+}$ (k = 3,4) isomers at the B3LYP/BS2+SMD(CH3CN)// B3LYP/BS2 level of theory. Concentration corrections for G were included.

Species	E (E_h)	G_{corr} (E_h)	G (E_h)	ΔG (kcal mol^{-1})
3b.H_6	–3443.463139	0.826327381	-3442.636812	0.0
(3b.H_6)b	–3443.4606	0.826688087	-3442.633912	1.8
(3b.H_6)c	–3443.449095	0.830587104	-3442.618507	11.5
(3b.H_6)d	–3443.437828	0.823588427	-3442.61424	14.2
(3b.H_6)e	–3443.427664	0.821326452	-3442.606338	19.1
(3b.H_6)f	–3443.417581	0.823433763	-3442.594147	26.8
3b.H_8	–3445.559802	0.846063308	-3444.713739	0.0
(3b.H_8)b	–3445.555313	0.846983416	-3444.70833	3.4

S11. $[Nb_2(P^{Me}{}_2N^{Me}{}_2)_4(H_2)_k]^{4+}$ (k = 0-2) Isomers

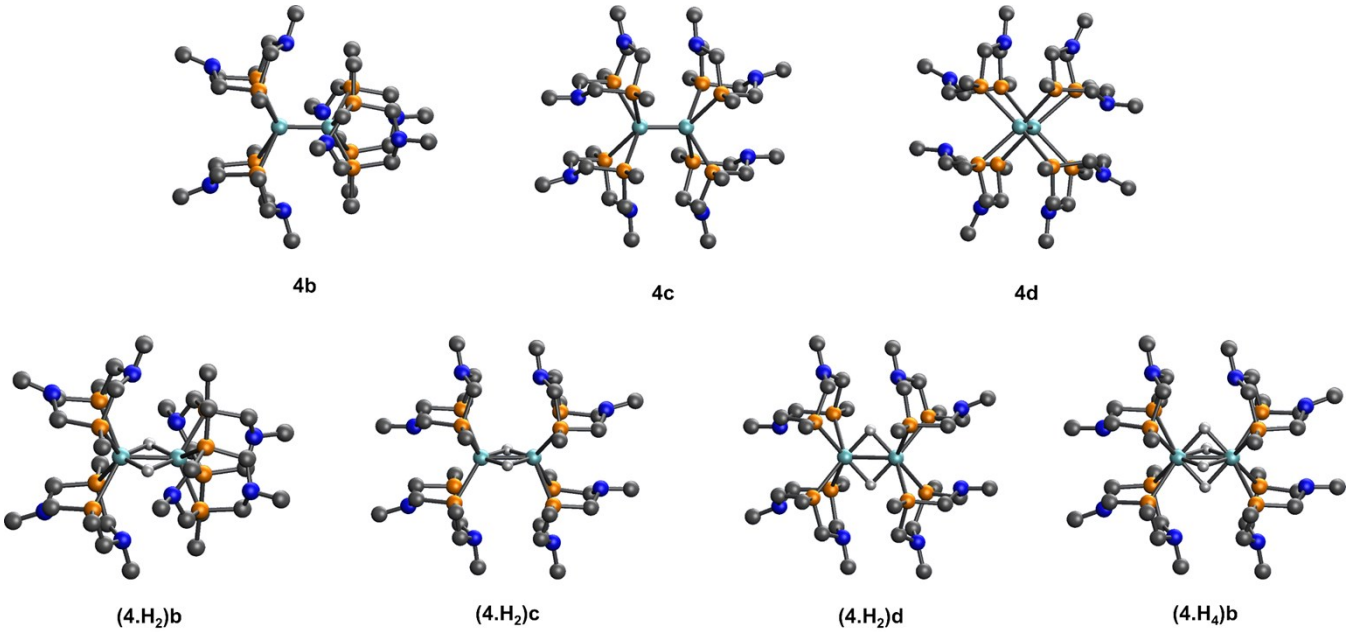

Figure S9. Ranking of low-lying free energy isomers of $[Nb_2(P^{Me}{}_2N^{Me}{}_2)_4(H_2)_k]^{4+}$ (k = 0-2) calculated in acetonitrile at the B3LYP/BS2+SMD(CH3CN)//B3LYP/BS2 level of theory. Spectator hydrogen atoms are omitted for clarity.

Table S13. Thermochemistry of distinct $[Nb_2(P^{Me}{}_2N^{Me}{}_2)_4H_k]^{4+}$ (k = 0,2,4) isomers at the B3LYP/BS2+SMD(CH3CN)// B3LYP/BS2 level of theory. Concentration corrections for G were included.

Species	E (E_h)	G_{corr} (E_h)	G (E_h)	ΔG (kcal mol^{-1})
4b	–4549.844095	1.042162	-4548.801933	0.0
4c	–4549.825028	1.038392	-4548.786636	+9.6
4d	–4549.778176	1.041017	-4548.737159	+40.6
(4.H_2)b	–4551.073369	1.055535	-4550.017834	0.0
(4.H_2)c	–4551.069011	1.054884	-4550.014127	+2.3
(4.H_2)d	–4551.048281	1.053451	-4549.994829	+14.4
4.H_4	–4552.291106	1.069766	-4551.221340	0.0
(4.H_4)b	–4552.281696	1.070873	-4551.210823	+6.6

S12. $[Nb_2(P^{Me}{}_2N^{Me}{}_2)_4(H_2)_k]^{4+}$ (k = 3,4) Isomers

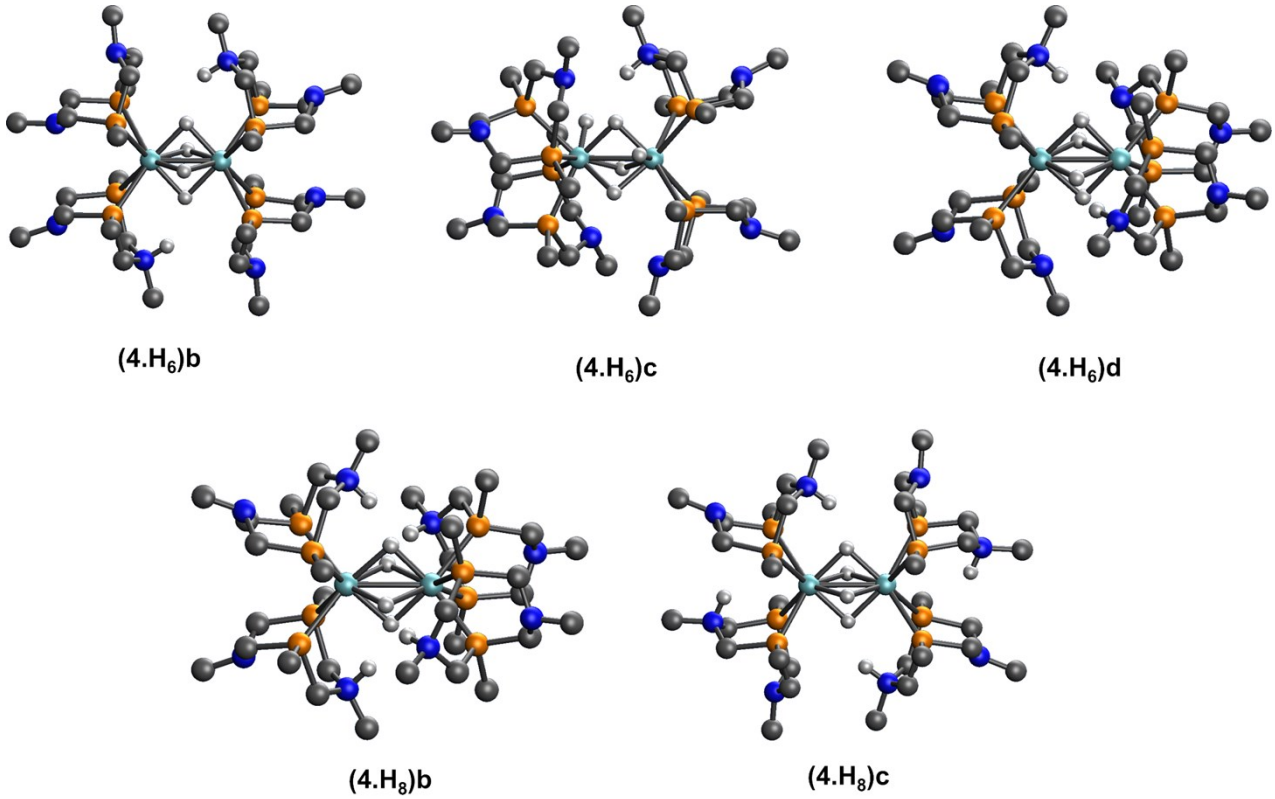

Figure S10. Ranking of low-lying free energy isomers of $[Nb_2(P^{Me}{}_2N^{Me}{}_2)_4(H_2)_k]^{4+}$ (k = 3,4) calculated in acetonitrile at the B3LYP/BS2+SMD(CH3CN)//B3LYP/BS2 level of theory. Spectator hydrogen atoms are omitted for clarity.

Table S14. Thermochemistry of distinct $[Nb_2(P^{Me}{}_2N^{Me}{}_2)_4(H_2)_k]^{4+}$ (k = 3,4) isomers at the B3LYP/BS2+SMD(CH3CN)// B3LYP/BS2 level of theory. Concentration corrections for G were included.

Species	E (E_h)	G_{corr} (E_h)	G (E_h)	ΔG (kcal mol^{-1})
4.H_6	–4553.496356	1.099217	-4552.400151	0.0
(4.H_6)b	–4553.488067	1.097064	-4552.394015	+3.9
(4.H_6)c	–4553.480312	1.093769	-4552.389555	+6.6
(4.H_6)d	–4553.447958	1.097447	-4552.353522	+29.3
4.H_8	–4554.645891	1.125313	-4553.523590	0.0
(4.H_8)b	–4554.635758	1.124974	-4553.513797	+6.1
(4.H_8)c	–4554.618779	1.122282	-4553.499508	+15.1

S13. Molecular Structures of Experimentally Known Diniobium Systems

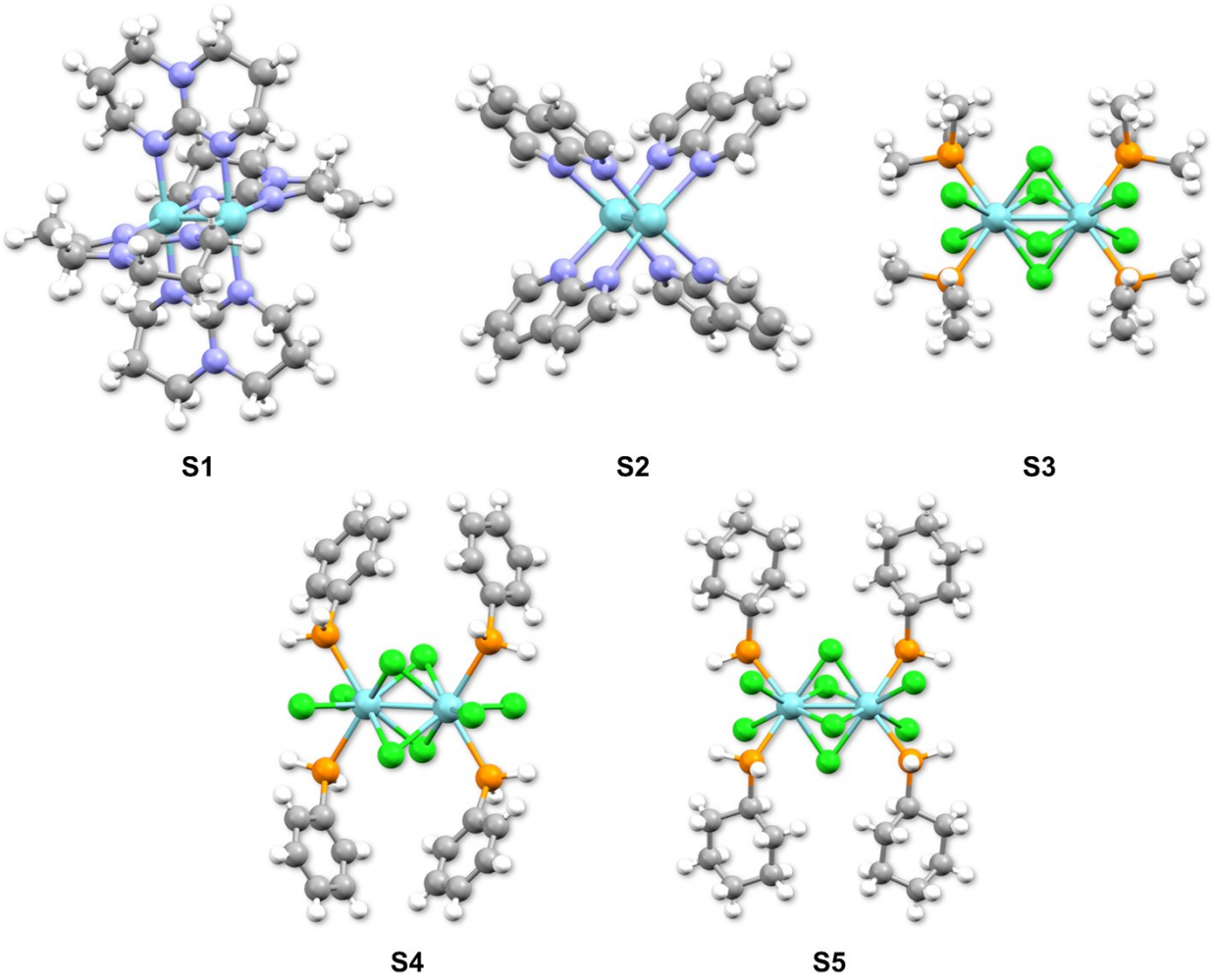

Figure S11. Optimized structures (B3LYP-D3(BJ)def2-SVP) of selected experimentally characterized diniobium systems. Selected geometrical parameters are given in Table S14 along with the relevant literature. Coloring scheme: Nb, cyan; N, blue; P, orange; Cl, green, C, grey, H, white.

Table S15. Calculated molecular structures (B3LYP-D3(BJ)def2-SVP) of experimentally known diniobium systems. Distances are in Å.

S1	Calc.	Exp.[S9]	% Deviation
Nb–Nb	2.198	2.203	0.25
Nb–N	2.221	2.199	1.0
S2	**Calc.**	**Exp.**[S10]	**% Deviation**
Nb–Nb	2.245	2.263	0.80
Nb–N (a)	2.298	2.240	2.6
Nb–N (b)	2.183	2.198	0.68
S3	**Calc.**	**Exp.**[S11]	**% Deviation**
Nb–Nb	2.840	2.836	0.14
Nb–Cl (a)	2.579	2.545	1.3
Nb–Cl (b)	2.514	2.506	0.32
Nb–P	2.681	2.675	0.22
S4	**Calc.**	**Exp.**[S12]	**% Deviation**
Nb–Nb	2.798	2.795	0.11
Nb–Cl (a)	2.554	2.523	1.2
Nb–Cl (b)	2.601	2.553	1.9
Nb–Cl (c)	2.501	2.496	0.20
Nb–P (a)	2.633	2.633	0.00
Nb–P (b)	2.645	2.634	0.42
S5	**Calc.**	**Exp.**[S12]	**% Deviation**
Nb–Nb	2.811	2.809	-0.07
Nb–Cl (a)	2.586	2.541	-1.77
Nb–Cl (b)	2.591	2.545	-1.81
Nb–Cl (c)	2.502	2.486	-0.64
Nb–P (a)	2.621	2.617	-0.15
Nb–P (b)	2.624	2.613	-0.42

References

[S1] M. Valiev, E. J. Bylaska, N. Govind, K. Kowalski, T. P. Straatsma, H. J. J. Van Dam, D. Wang, J. Nieplocha, E. Apra, T. L. Windus and W. A. de Jong, *Comput. Phys. Commun.*, 2010, **181**, 1477–1489.

[S2] (a) S. H. Vosko, L. Wilk and M. Nusair, *Can. J. Phys.*, 1980, **58**, 1200–1211; (b) C. Lee, W. Yang and R. G. Parr, *Phys. Rev. B*, 1988, **37**, 785–789; (c) A. D. Becke, *J. Chem. Phys.*, 1993, **98**, 5648–5652; (d) P. J. Stephens, F. J. Devlin, C. F. Chabalowski and M. J. Frisch, *J. Phys. Chem.*, 1994, **98**, 11623–11627.

[S3] (a) R. Ditchfield, W. J. Hehre and J. A. Pople, *J. Chem. Phys.*, 1971, **54**, 724–728; (b) W. J. Hehre, R. Ditchfield and J. A. Pople, *J. Chem. Phys.*, 1972, **56**, 2257–2261; (c) P. C. Hariharan and J. A. Pople, *Theor. Chim. Acta*, 1973, **28**, 213–222; (d) M. M. Francl, W. J. Pietro, W. J. Hehre, J. S. Binkley, M. S. Gordon, D. J. DeFrees and J. A. Pople, *J. Chem. Phys.*, 1982, **77**, 3654–3665; (e) M. S. Gordon, J. S. Binkley, J. A. Pople, W. J. Pietro and W. J. Hehre, *J. Am. Chem. Soc.*, 1982, **104**, 2797–2803.

[S4] (a) D. Andrae, U. Häußermann, M. Dolg, H. Stoll and H. Preuß, *Theor. Chim. Acta*, 1990, **77**, 123–141; (b) J. M. L. Martin and A. Sundermann, *J. Chem. Phys.*, 2001, **114**, 3408–3420.

[S5] A. V. Marenich, C. J. Cramer and D. G. Truhlar, *J. Phys. Chem. B*, 2009, **113**, 6378–6396.

[S6] A. T. B. Gilbert, *IQmol Molecular Viewer*, Available at: http://iqmol.org. 2013.

[S7] F. L. Hirshfeld, *Theor. Chim. Acta*, 1977, **44**, 129–138.

[S8] T. Lu and F. Chen, *J. Comput. Chem.*, 2012, **33**, 580–592.

[S9] F. A. Cotton, J. H. Matonic and C. A. Murillo, *J. Am. Chem. Soc.*, 1997, **119**, 7889–7890.

[S10] F. A. Cotton, J. H. Matonic and C. A. Murillo, *J. Am. Chem. Soc.*, 1998, **120**, 6047–6052.

[S11] F. A. Cotton, S. A. Duraj and W. J. Roth, *Inorg. Chem.*, 1984, **23**, 3592–3596.

[S12] J. T. Scheper, K. C. Jayaratne, L. M. Liable-Sands, G. P. A. Yap, A. L. Rheingold and C. H. Winter, *Inorg. Chem.*, 1999, **38**, 4354–4360.